AC-DC LOAD FLOW WITH UNIT-CONNECTED GENERATOR-CONVERTER INFEEDS

J. Arrillaga, Fellow; C.P. Arnold, Sen. Member
University of Canterbury, Christchurch, New Zealand

J.R. Camacho, Student Member
Universidade Federal de Uberlandia, Brazil

S. Sankar, Non-member
University of Canterbury, Christchurch, New Zealand

Abstract - It is demonstrated that the conventional ac-dc formulation is not directly applicable to the unit-connected generator-converter. Alternative steady state models are derived which are considered reasonable for cylindrical rotor machines but not for salient-pole generators. Finally an accurate algorithm of general applicability, called the *Equivalent Inverter*, is proposed which uses unit-connection characteristics derived from a time domain simulation.

INTRODUCTION

The connection of remote power generating plant via long distance HVdc transmission has already been proved extremely reliable in many projects. In an attempt to simplify the conventional design, the use of unit connected generators is being seriously considered at present[1-4]. CIGRÉ Working Group WG 14.09 is also investigating the unit connection.

Earlier references on this topic have discussed the potential cost savings and operational reliability of the unit-connected generator-HVdc converters in isolation from the receiving end power system. However final technical and economical comparisons with the conventional configuration will need to consider the overall system performance. In particular, the effect of the alternative scheme in power transmission capability and system stability must be carefully assessed.

Although the ac-dc load flow is well understood[5], some of the basic assumptions made in its formulation have been found inapplicable to the unit-connected configuration[6].

This paper establishes the modifications required for the continued use of the conventional ac-dc load flow formulation and then describes a more general and accurate algorithm, based on the use of converter characteristics derived from dynamic simulation.

THE CONVENTIONAL AC-DC LOAD FLOW FORMULATION

With reference to fig. 1 and the per unit system[5], the following relationships exist between the variables involved in the static conversion process:

$$I_s = k\frac{3\sqrt{2}}{\pi} I_d \tag{1}$$

$$I_p = aI_s \tag{2}$$

$$V_d = \frac{3\sqrt{2}}{\pi} a V_{term}\cos\alpha - \frac{3}{\pi}X_c I_d \tag{3}$$

$$V_d I_d = E I_s \cos\varphi \tag{4}$$

$$V_d I_d = V_{term} I_p \cos\phi \tag{5}$$

92 SM 593-4 PWRS A paper recommended and approved by the IEEE Power System Engineering Committee of the IEEE Power Engineering Society for presentation at the IEEE/PES 1992 Summer Meeting, Seattle, WA, July 12-16, 1992. Manuscript submitted August 26, 1991; made available for printing May 22, 1992.

$$I_s = B_t \sin\varphi - B_t a V_{term} \sin\phi \tag{6}$$

$$f(V_d, I_d) = 0 \tag{7}$$

where B_t is the converter transformer leakage susceptance and k in equation (1) is very close to unity.

Since the bus between the converter and the transformer is not required, equations (1), (2), (4) and (5) can be combined and the terminal ac busbar voltage (V_{term}) used as a reference. A reduced set of variables and equations results[5] suitable for investigating the effect of control strategies in current use. The set of variables is:

$$\bar{x} = [V_d, I_d, a, \cos\alpha, \phi]^T \tag{8}$$

Each converter terminal is therefore represented by a five variable set of non-linear equations, which are then combined with the ac system equations and solved using either simultaneous or sequential iterative algorithms[5].

Adaptation for use with the unit-connection.

In the absence of filters the voltage at the converter terminal is not sinusoidal and can not be used as the commutating voltage in the conventional formulation. Instead, the use of the generator internal EMF behind sub-transient reactance (E'') is commonly accepted.

In the case of a non-salient rotor machine the load flow formulation described in the previous section should be applicable by shifting the converter interface to a fictitious terminal (the internal EMF behind sub-transient reactance) where the waveform is assumed sinusoidal.

Although E'' is neither accessible nor directly controllable and varies with the load, its magnitude can be derived from the generator's sub-transient phasor diagram for the nominal operating point and then kept constant (as shown by dotted lines in fig. 2). This is done to satisfy the generator's conventional load flow specification (i.e. constant voltage) but at the fictitious internal E'' bus. The conventional load flow is then carried out on the assumption of perfect filtering at that point.

With salient-pole generators the conventional formulation is often used by averaging the sub-transient reactances, i.e. $X''=(X_d''+X_q'')/2$. So far the error of such an approximation has not been discussed, due to the vast number of variables that contribute to differences between steady state and dynamic related formulations.

In the case of unit-connected generation, tappings are not required on the transformer and hence the variable a must be maintained at its nominal value.

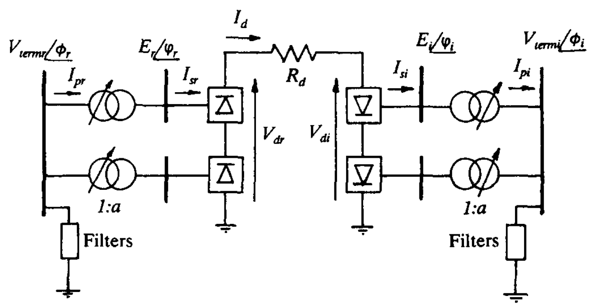

Fig. 1. Typical HVdc system.

0885-8950/93$03.00 © 1992 IEEE

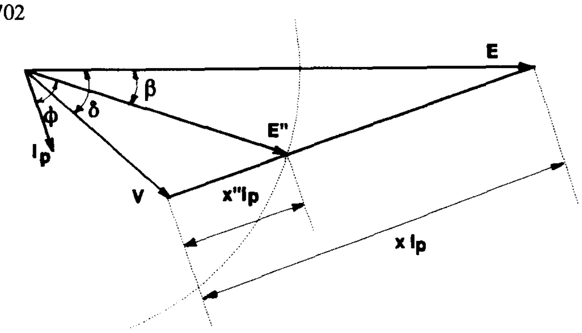

Fig. 2. Simplified phasor diagram of the unit-connected generator.

Modified Algorithm for Varying Commutating Voltages.

As already indicated, the internal EMF behind sub-transient reactance is not directly controllable. Instead, the generator excitation will be controlled to provide the specified dc link power at the specified firing angle (α_{min}).

Therefore the commutating voltage (E'') is not known in advance and its magnitude and phase angle (β) must be derived as part of the iterative solution.

The conventional vector equation (8) is replaced by:

$$\bar{x} = [V_d , I_d , \cos\alpha , \phi , E , E'' , \beta]^T \tag{9}$$

Therefore seven residual equations are needed to formulate the load flow problem at the rectifier end.

The first two equations are common to the conventional model (with the tap ratio variable removed). Therefore:

$$R(1) = V_d - k_1 E'' \cos\phi \tag{10}$$

$$R(2) = V_d - k_1 E'' \cos\alpha - \frac{3}{\pi} X_c I_d \tag{11}$$

where $k_1 = 3\surd 2/\pi$.

The next two are derived from the generator sub-transient phasor diagram of fig. 2. That is:

$$R(3) = E - E'' \cos\beta - (x - x'') \mid I_p \mid \sin(\beta + \phi) \tag{12}$$

$$R(4) = E'' \sin\beta - (x - x'') \mid I_p \mid \cos(\beta + \phi) \tag{13}$$

To complete the set, three control specifications are required, a typical selection being:

$$R(5) = I_d - I_d^{sp} \tag{14}$$

$$R(6) = E - E^{sp} \tag{15}$$

$$R(7) = \cos\alpha - \cos\alpha_{min} \tag{16}$$

LOAD FLOW MODEL BASED ON DYNAMIC SIMULATION.

Accurate Derivation of Rectifier Characteristics.

In the absence of local load at the rectifier end, the unit-connected scheme can be considered as an equivalent HVdc generator and the complete HVdc link as an equivalent inverter.

A time domain solution of the differential equations representing the generator and rectifier behaviour provides detailed information of the required voltage and current waveforms. Once the steady state waveforms are obtained, their averaged values provide accurate output characteristics for the unit-connected group. For every combination of I_d and α the output dc voltage V_d is calculated and the resulting information is stored in memory for use in the load flow solution.

Two charts have been stored in this case. The first is for the V_d/I_d characteristic with the rectifier operating as a diode bridge (α = 0°). 15 points have been used to adequately model the characteristic. The second chart is for the V_d/α characteristic with the rectifier operating under constant current control (I_d = 1.0 kA) and in this case 10 points have been used.

This is a very demanding exercise that requires approximately 30 minutes of CPU time using a VAX 3500 computer for each point of the characteristic. However it only needs to be carried out once for a particular HVdc system.

The type of interpolation used is a variation of the method of divided differences[7] with the degree of the interpolation being constrained to a second order. This method was chosen because it requires less arithmetic operations, points can be simply added or subtracted from the set used to construct the polynomial and also previous computations can be reused.

The Equivalent Inverter Model

The absence of tap changers and the irrelevance of ϕ at the generator terminals of the unit connection scheme permits a simpler formulation, in the form of a modified *Equivalent Inverter.*

In this case the vector of variables is:

$$\bar{x} = [V_d , I_d , a , \cos\alpha , \phi , \cos\gamma]^T \tag{17}$$

which contains the five variables of the conventional (inverter) set and an extra variable (*cos* α) representing the rectifier end of the link. A schematic diagram of the *Equivalent Inverter* is shown in fig. 3.

In line with conventional practice the *Equivalent Inverter* will normally be on extinction angle control (γ^{sp}_{min}) and the rectifier on current control, the specified current level derived from a constant power setting (P_d^{sp}) at the inverter end.

Besides P_d^{sp} and γ^{sp}_{min} a third control specification must be made to match the six-variable formulation. It is suggested that α^{sp}_{min} is used and the inverter transformer tap freed. This provides for the highest transmission voltage. Should the tap changer attempt to violate one of its limits, this limit becomes the new control specification while freeing the value of α.

The complete set of residual equations becomes:

$$R(1) = V_d - k_1\, a\, V_{term} \cos\phi \tag{18}$$

$$R(2) = V_d - k_1\, a\, V_{term} \cos(\pi - \gamma) - \frac{3}{\pi} X_c I_d \tag{19}$$

$$R(3) = V_d + R_d I_d - f(I_d , \alpha) \tag{20}$$

$$R(4) = V_d I_d - P_{dc}^{sp} \tag{21}$$

$$R(5) = \cos(\pi - \gamma) - \cos(\pi - \gamma^{sp}) \tag{22}$$

$$R(6) = \cos\alpha - \cos\alpha_{min} \tag{23}$$

The incorporation of the equivalent inverter in a Fast Decoupled ac-dc load flow algorithm[5] requires modifications to the B", AA', AA" and BB" sub-matrices of the Jacobian matrix. These sub-matrices, shown in Appendix B, are greatly simplified as they contain only a single element each.

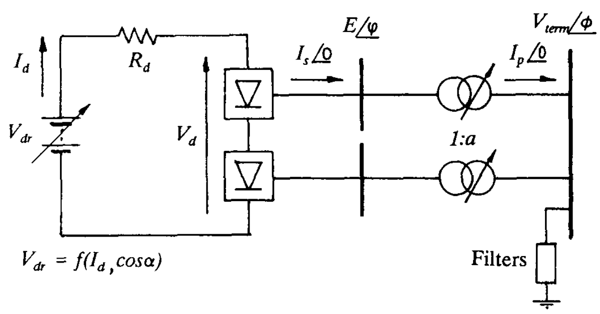

Fig. 3. The Equivalent Inverter.

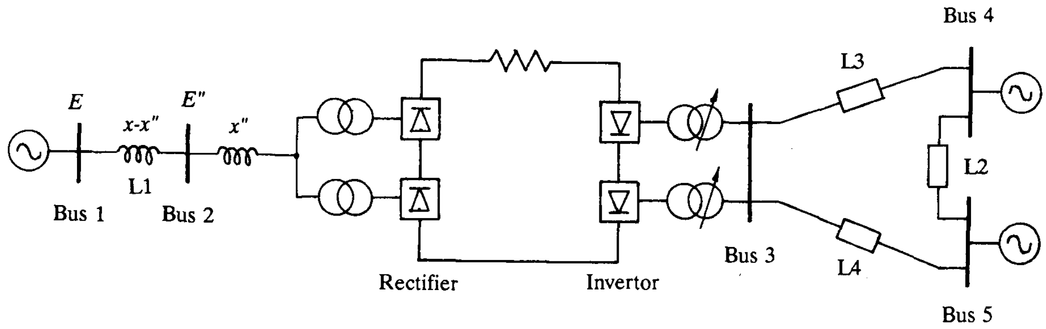

Fig. 4. The test system.

PERFORMANCE OF THE ALGORITHMS

Test System

The test system consists of a single unit connected generator, an HVdc link with a 12 pulse converter and a 3 busbar receiving end ac system, as shown in fig. 4. All other relevant information is given in Appendix A.

Conventional Load Flow Results (Model 1)

In order to obtain the linear V_d/I_d characteristic of a conventional HVdc scheme, the generator excitation must be controlled to keep the commutating voltage (E'') constant at some specified value to provide the required nominal dc voltage at minimum delay angle (α_{min}). The V_d/I_d characteristic is shown in fig. 5.

By way of an example, the sending end of the test system can be operated as a diode rectifier ($\alpha=0°$) with an averaged sub-transient reactance and a constant E'' (of 66.66 kV). The results of varying the constant current specification from 0.5 to 0.9 kA are shown in Table 1. The table includes the calculated tap position of the inverter end transformer needed to maintain a constant minimum extinction angle of $\gamma_{min}=18°$. The complex powers at the three busbars of the ac system are also shown.

The results for a current setting of 0.9 kA cannot be included because of a violation of the maximum commutation angle of 30°. This indicates the inapplicability of the conventional formulation in all but a limited set of circumstances.

Modified Steady State (Model 2) and Equivalent Inverter (Model 3) Results

In order to highlight the limitations of the steady state formulation two examples have been chosen, one with varying dc current and minimum firing angle (α_{min}) and the other with variable α and a constant link current setting. In both cases the generator excitation is kept constant at the value necessary to achieve the nominal dc voltage of 80.0 kV when the nominal link current is 1.0 kA. Therefore in all cases the specified variables are E, I_d and α. The identical excitations are confirmed in fig. 5 for zero dc current.

Tables 2 and 3 illustrate the major differences between the conventional steady state formulation and the accurate solution based on dynamic simulation characteristics. At the lower end of the current setting range (i.e. below 0.7 kA), the tables show that the arbitrary maximum transformer tap setting of 20% is exceeded when using the conventional formulation, whereas this is not the case in the equivalent inverter results. From 0.7 to 0.9 kA, differences of 30% occur in the calculated values of the inverter tap position and 8% in the calculated values of complex power in the ac system. Further increases in current setting result in violations of the commutation angle limit and thus invalidate any results obtained from the steady state. On the other hand the equivalent inverter shows that minimum extinction angle is still maintained at current settings in excess of 1.0 kA and that changeover from tap to γ control takes place at a current less than 1.25 kA. Although the commutation angle cannot be determined in the case of the equivalent inverter model, the results from the dynamic simulation are valid for angles above and below 30°.

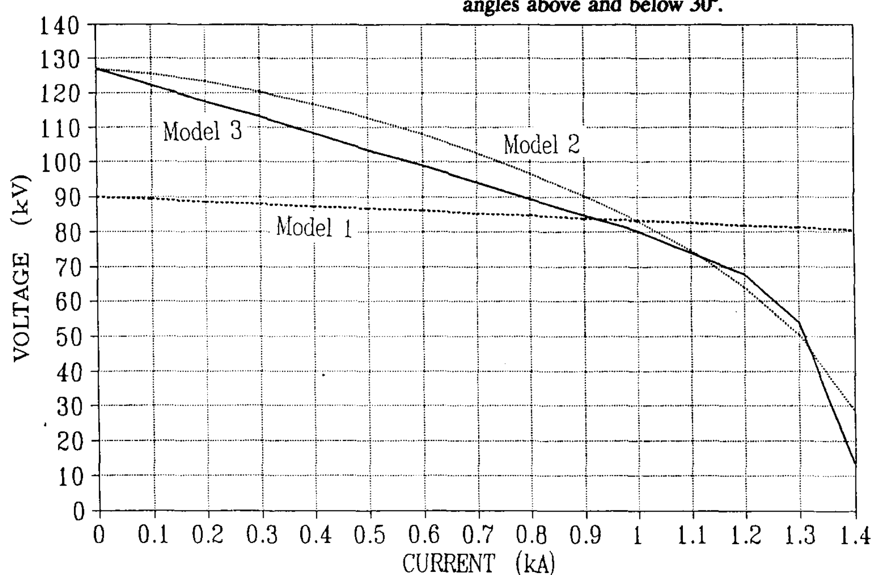

Fig. 5. Dc voltage / dc current characteristics for 3 models of the unit-connected HVdc generator- converter.

Table 1 Conventional load-flow (Model 1). Diode rectifier bridge ($\alpha=0°$). $\gamma_{min}=18°$. With a in %, P in MW and Q in MVAr.

			Bus 3		Bus 4		Bus 5	
$I_d(kA)$	γ_i	a_i	P_3	Q_3	P_4	Q_4	P_5	Q_5
0.50	γ_{min}	-10.59	43.07	-15.43	-140.	9.87	96.93	9.25
0.60	γ_{min}	-10.02	51.22	-18.69	-140.	11.49	88.78	10.79
0.70	γ_{min}	-9.44	59.21	-21.99	-140.	13.16	80.79	12.37
0.80	γ_{min}	-8.85	67.05	-25.36	-140.	14.86	72.95	14.00
0.85	γ_{min}	-8.55	70.91	-27.06	-140.	15.73	69.09	14.83
0.90	$\mu_r > 30°$							

Table 2 Modified load-flow (Model 2). Diode rectifier bridge ($\alpha=0°$). $\gamma_{min}=18°$. With a in %, P in MW and Q in MVAr.

			Bus 3		Bus 4		Bus 5	
$I_d(kA)$	γ_i	a_i	P_3	Q_3	P_4	Q_4	P_5	Q_5
0.70	$a_i < -20\%$							
0.80	γ_{min}	-19.99	76.83	-28.57	-140.	16.50	63.17	15.57
0.85	γ_{min}	-17.71	78.91	-29.68	-140.	17.07	61.09	16.12
0.90	γ_{min}	-14.76	80.52	-30.67	-140.	17.58	59.48	16.61
1.00	$\mu_r > 30°$							
1.25	$\mu_r > 30°$							

Table 3 Equivalent Inverter (Model 3). Diode rectifier bridge ($\alpha=0°$). $\gamma_{min}=18°$, a_{max} = 20%. With γ in degrees, a in %, P in MW and Q in MVAr.

			Bus 3		Bus 4		Bus 5	
$I_d(kA)$	γ_i	a_i	P_3	Q_3	P_4	Q_4	P_5	Q_5
0.70	γ_{min}	-18.93	66.22	-24.00	-140.	14.32	73.78	13.47
0.80	γ_{min}	-14.82	71.81	-26.60	-140.	15.66	68.19	14.76
0.85	γ_{min}	-12.61	74.25	-27.82	-140.	16.29	65.75	15.37
0.90	γ_{min}	-10.27	76.44	-28.98	-140.	16.89	63.56	15.95
1.00	γ_{min}	-5.19	80.10	-31.13	-140.	17.99	59.90	17.04
1.25	23.06	a_{max}	75.37	-38.62	-140.	21.82	64.63	20.89

The second example is used to illustrate the effect of firing angle variation on the inverter tap, extinction angle and rectifier commutation angle; the results are given in Table 4. The differences in the first row ($\alpha_{min}=0°$) have already been discussed in the previous example. For firing angles between 5 and 20° both algorithms show a similar pattern but differences of 6.5% are observed in the values of commutation overlap. For $\alpha=30°$ only Model 2 show a changeover from γ to tap control. For 45° and beyond, all models predict tap control, the actual values of γ differing by up to 33%.

From the above results and discussion it is clear that only the *Equivalent Inverter* algorithm can be relied upon to provide realistic load flow information when the system contains unit connected in-feeds.

Table 4 Results with I_d = 1.0 kA and variable α. $\gamma_{min}=18°$, a_{max} = 20%.

α	Model 1			Model 2			Model 3		
---	a_i	γ_i	μ_r	a_i	γ_i	μ_r	a_i	γ_i	μ_r
0°	$\mu_r > 30°$						-5.19	γ_{min}	28.98
5°	-7.26	γ_{min}	27.19	-6.71	γ_{min}	27.29	-3.21	γ_{min}	26.1
10°	-6.11	γ_{min}	24.40	-3.97	γ_{min}	23.73	0.31	γ_{min}	22.6
20°	-1.23	γ_{min}	17.84	6.66	γ_{min}	18.86	4.85	γ_{min}	17.7
30°	7.90	γ_{min}	14.27	a_{max}	23.46	15.97	19.05	γ_{min}	15.15
45°	a_{max}	31.93	11.14	a_{max}	48.07	13.60	a_{max}	41.30	12.7
50°	a_{max}	40.15	10.48	a_{max}	54.31	13.12	a_{max}	47.56	12.33
65°	a_{max}	61.75	9.18	a_{max}	70.73	12.22	a_{max}	66.38	11.41
80°	a_{max}	81.81	8.64	a_{max}	85.46	11.87	a_{max}	85.90	11.07

CONCLUSIONS

The conventional ac-dc steady state formulation has been modified to analyse HVdc load flows with unit connected generator converter in-feeds. However the steady state algorithm is restricted in its application to large power conditions due to the large commutation overlap caused by the extra reactance of the unit connection.

Also the results have been shown to be in considerable error when the generators contain rotor saliency (probably the most common case for remote generating plant).

A new concept, called the *Equivalent Inverter* which uses unit connection characteristics derived from time domain simulation, has been presented as a practical alternative for general load flow studies involving unit connected schemes.

ACKNOWLEDGEMENTS.

The authors wish to acknowledge the financial assistance provided by New Zealand Ministry of External Relations and Trade, by The Universidade Federal de Uberlandia and by the Capes /Ministry of Education of Brazil. They also acknowledge the advice received from their colleagues Dr. N.R. Watson, and Messrs. A. Medina, M. Zavahir and M. Villablanca.

REFERENCES.

[1] - P.C.S. Krishnayya, et al., "A Review of Unit Generator-Converter Connections for HVdc Transmission", IEEE/CSEE Joint Conference on High Voltage Transmission Systems, Beijing, China, 1987.

[2] - K.W. Kangiesser, "Unit Connection of Generator and Converter to be Integrated in HVdc or HVac Energy Transmission", International Symposium on HVdc Technology, Rio de Janeiro, Brazil, 1983.

[3] - M. Naidu and R.M. Mathur, "Evaluation of Unit Connected, Variable Speed, Hydropower Station for HVdc Power Transmission", Trans. IEEE, vol. PS-5, no. 2, 1989, pp. 668-76.

[4] - J.P. Bowles, "Multiterminal HVdc Transmission Systems Incorporating Diode Rectifier Stations", Trans. IEEE, vol. PAS-100, no. 4, 1981, pp. 1674-8.

[5] - J. Arrillaga, C.P. Arnold and B.J. Harker, "Computer Modelling of Electrical Power Systems", J. Wiley & Sons Ltd., London, 1983.

[6] - J. Arrillaga, S. Sankar, N.R. Watson and C.P. Arnold, "Operational Capability of Generator-HVdc Converter Units", Trans. IEEE, Winter Meeting 1991, paper 91WM 120-6 PWRD.

[7] - F.C. Gerald and P.O. Wheatley, "Applied Numerical Analysis", Addison-Wesley Publishing Co., New York, 1985.

APPENDIX A. - Test System Data

All parameters quoted are in per unit on a 100 MVA base except where otherwise specified.

Salient Pole Generator:

Rating:	100 MVA
Terminal Voltage:	13.8 kV
D-axis reactance:	1.2
Q-axis reactance:	0.8
D-axis sub-transient reactance:	0.2
Q-axis sub-transient reactance:	0.367

Dc Link:

Type:	12 pulse
Nominal Current:	1.0 kA
Nominal Voltage:	80.0 kV
Resistance:	1.0 Ω

Converter Transformer:

Rating:	50 MVA
Reactance:	0.1
Voltage:	13.8/30.36 kV

System branch impedances:

L1:	j0.9165
L2:	j0.04
L3:	j0.03
L4:	j0.03

Initial conditions:

Bus 1:	Slack	V=1.548 pu	
Bus 2:	P,Q		
Bus 3:	Slack	V=1.0 pu	
Bus 4:	P,V	V=1.0 pu	P=-140.0 MW
Bus 5:	P,Q		

APPENDIX B - Equivalent Inverter ac-dc Jacobian Matrices.

$$\begin{bmatrix} \vdots \\ \Delta P / V \\ \vdots \\ \hline \Delta P / V_{term} \\ \hline R \end{bmatrix} = \begin{bmatrix} B' & \\ & \\ & AA' \\ & A \end{bmatrix} \begin{bmatrix} \vdots \\ \Delta\theta \\ \vdots \\ \hline \Delta\theta \\ \hline \Delta x \end{bmatrix}$$

$$\begin{bmatrix} \vdots \\ \Delta Q / V \\ \vdots \\ \hline \Delta Q / V_{term} \\ \hline R \end{bmatrix} = \begin{bmatrix} B'' & & \\ & B''_{ii} & AA'' \\ & BB'' & A \end{bmatrix} \begin{bmatrix} \vdots \\ \Delta V \\ \vdots \\ \hline \Delta V_{term} \\ \hline \Delta x \end{bmatrix}$$

The elements of the dc Jacobian matrix $[A]$ are:

$$[A] = \begin{bmatrix} 1 & & -k_1 V_{term} \cos\phi & & k_1 a\, V_{term} \sin\phi & \\ 1 & \frac{-3}{\pi} X_c & -k_1 V_{term} \cos(\pi-\gamma) & & k_1 a\, V_{term} & \\ 1 & R_d + \frac{\delta V_{dr}}{\delta I_d} & & \frac{\delta V_{dr}}{\delta I_d} & & \\ I_d & V_d & & & & \\ & & & & & -1 \\ & & & 1 & & \end{bmatrix}$$

where $Vd_r = f(Id, \cos\alpha)$
and with rows ordered as in equations (18)-(23) and columns ordered as in equation (17).

Also:

$$[AA'] = [\ \delta P_{term}(dc) / \delta x\ ] / V_{term}$$

$$[AA''] = [\ \delta Q_{term}(dc) / \delta x\ ] / V_{term}$$

$$[BB''] = \delta R / \delta V_{term}$$

APPENDIX C - List of Symbols

- E - internal EMF,
- E'' - commutating voltage,
- X - generator contribution to the commutation voltage,
- X'' - generator sub-transient reactance,
- X_t - converter transformer reactance,
- X_c - commutating reactance of the converter,
- I_d - Dc current of the link,
- I_p - Ac current of the primary of the converter transformer,
- I_s - Ac current of the secondary of the converter transformer,
- a - tap of the converter transformer,
- V_d - Dc voltage of the converter,
- V_{term} - Ac voltage of the primary of the converter transformer,
- $E_{r,i}$ - Ac voltage of the secondary of the converter transformer,
- α - firing angle of the converter,
- γ - extinction angle of the converter,
- u - commutation angle of the converter,
- ϕ - power factor angle in the primary of converter transformer,
- φ - power factor angle in the secondary of converter transformer,
- r - rectifier,
- i - inverter.

Jos Arrillaga received his BE degree of Spain and his MSc, PhD and Dsc of Manchester, where he led the power systems group of UMIST between 1970-74. He has been a Professor at the University of Canterbury since 1975. He is a Fellow of the IEE, IEEE, the New Zealand Institution of Engineers and the Royal Society of New Zealand.

Chris Arnold obtained his Msc and PhD from UMIST in 1970 and 1976 and between these events worked with G.E. in Schenectady, NY, USA. Since 1976 he has worked as a Lecturer and Senior Lecturer at the University of Canterbury, Christchurch, New Zealand. Dr. Arnold is a Member of IEE, a Senior Member of the IEEE, a Chartered Engineer of the U.K. and a Registered Engineer of N.Z.

J.R. Camacho received his BE degree from Universidade Federal de Uberlandia (UFUb) - Brazil in 1978, his MSc from Universidade Federal de Santa Catarina (UFSC) - Brazil in 1987. Currently he is on leave as a Lecturer at UFUb-Brazil working on his PhD at the University of Canterbury, Christchurch, N.Z. Mr. Camacho is a Student Member of the IEEE and a Registered Engineer of Brazil.

S. Sankar received his BE degree from Madras University in 1982, his M.Tech. from the Indian Institute of Technology, Bombay of 1984 and his PhD from the University of Canterbury, N.Z. in 1991. Currently he is a Post-Doctoral Fellow at the University of Canterbury, N.Z.